JOURNAL OF AIRCRAFT
Vol. 31, No. 5, Sept.–Oct. 1994

Engineering Notes

ENGINEERING NOTES are short manuscripts describing new developments or important results of a preliminary nature. These Notes cannot exceed 6 manuscript pages and 3 figures; a page of text may be substituted for a figure and vice versa. After informal review by the editors, they may be published within a few months of the date of receipt. Style requirements are the same as for regular contributions (see inside back cover).

Continuous Gust Response and Sensitivity Derivatives Using State-Space Models

Arie Zole* and Mordechay Karpel†
Technion—Israel Institute of Technology, Haifa 32000, Israel

Introduction

AN atmospheric flight vehicle is exposed to air turbulence that causes time-varying aerodynamic loads. These continuous-gust loads, amplified by the aeroelastic response of the vehicle, may result in critical structural design conditions.[1] The response of the automatic flight control system to structural vibrations may also play an important role. Continuous-gust response is analyzed by aeroservoelastic models that include unsteady aerodynamic, control, and structural dynamics effects. The gusts caused by air turbulence are defined in statistical terms by their power spectral density (PSD) functions and root-mean-square (rms) values.

Classical frequency-domain methods calculate the structural response by first calculating the response to sinusoidal gusts, and then the associated response PSD at many frequency points. Numerical integration is then used to calculate the rms response values. Modern aeroservoelastic modeling techniques, which are based on constant-coefficient, time-domain, first-order (state-space) formulation[2] originally used for stability analysis, opened the way for a significantly more efficient way to analyze continuous gust response. The main difficulty of the state-space modeling is in the requirement for approximating the unsteady aerodynamic force coefficient matrices by rational functions of the Laplace variable. The resulting model contains aerodynamic states that represent the time lag in the development of the aerodynamic forces. The minimum-state (MS) approximation method,[3] and the procedure of physical weighting of the aerodynamic data,[4,5] were designed to minimize the number of aerodynamic states per desired accuracy. The aeroelastic states are augmented by gust filter states[6] in a way that results in a linear system excited by white noise. A matrix Lyapunov equation is then solved for the state covariance matrix that yields a direct solution for the rms responses.

The multidisciplinary nature of aeroservoelasticity requires an integrated approach in the design of modern flight vehicles.[7,8] A work was conducted to extend the MS analysis and the sensitivity derivatives of Ref. 8 to include continuous-gust response of realistic cases. Key equations and selected results are given in this Note.

Received Jan. 25, 1993; revision received August 24, 1993; accepted for publication Sept. 3, 1993.

*Graduate Student, Faculty of Aerospace Engineering.
†Associate Professor, Faculty of Aerospace Engineering. Member AIAA.

State-Space Equations of Motion

The most general rational approximation of the tabulated aerodynamic force coefficient (AFC) matrix $[Q(jk)] \equiv [Q_s(jk)Q_c(jk)Q_g(jk)]$ is[3]

$$[\bar{Q}(jk)] = [A_0] + [A_1]jk + [A_2](jk)^2 + [D](jk[I] - [R])^{-1}[E]jk \tag{1}$$

where k is the reduced frequency $\omega b/V$, where ω is the frequency of oscillations, b is a reference semichord, and V is the true airspeed. $[R]$ is a diagonal matrix of negative aerodynamic roots representing the time lag in the development of the unsteady aerodynamic forces. The approximation coefficient matrices, $[A_0]$, $[A_1]$, $[A_2]$, and $[E]$, can be column-partitioned (as $[Q(jk)]$) with the subscripts s, c, and g relating to structural, control, and gust columns, respectively. It can be shown[9] that all the commonly used rational-function approximations of the unsteady aerodynamics can be brought to the form of Eq. (1). In all these procedures, some of the matrix coefficients in Eq. (1) are predetermined or constrained, and the others are used as free approximation variables in least-square procedures that fit the tabulated AFC matrices. The MS method used in this work is the only one that uses both $[D]$ and $[E]$ of Eq. (1) as free approximation variables, which results in a nonlinear weighted least-square problem, but yields a minimal approximation order per desired accuracy. The steady part of $\bar{Q}(jk)$ in Eq. (1) is constrained to match the steady tabulated data, namely $[A_0] = [Q(0)]$. An imaginary-part data match constraint at a selected tabulated k_g is used to define $[A_1]$. A real-part data match constraint at a selected tabulated k_f is used to define $[A_2]$, except for the gust column in $[A_2]$ that is constrained to $\{A_{g_2}\} = \{\mathbf{0}\}$ to avoid a $\ddot{w}_g$ term in the time-domain model below.

The rational approximation is extended to the entire Laplace domain by replacing jk in Eq. (1) by sb/V. The resulting time-domain, state-space, closed-loop aeroservoelastic equation of motion is

$$\{\dot{\boldsymbol{x}}_p\} = [A_p]\{\boldsymbol{x}_p\} + [B_{w_p}]\{\boldsymbol{w}_p\} \tag{2}$$

where the state vector $\{\boldsymbol{x}_p\}$ includes modal structural displacements and velocities, aerodynamic lag states, and control states. The input vector is $\{\boldsymbol{w}_p\} = [w_g \dot{w}_g]^T$, where w_g is the gust velocity amplitude. The coefficient matrices in Eq. (2) are detailed in Refs. 4 and 9.

The outputs of the aeroelastic system are expressed by

$$\{\boldsymbol{y}_p\} = [C_p]\{\boldsymbol{x}_p\} + [D_{w_p}]\{\boldsymbol{w}_p\} \tag{3}$$

where structural displacements and velocities, and mode-displacement loads are expressed as functions of the states only, namely with $[D_{w_p}] = [0]$. Structural accelerations, and acceleration-dependent summation-of-forces loads have a nonzero $[D_{w_p}]$.

In order to facilitate the usage of Lyapunov equations for direct rms response solutions, it is desired to transform the gust-excited aeroservoelastic Eq. (2) into an equivalent one that is excited by white noise. This is achieved by designing

a gust filter $T_g(s)$ that, when excited by white noise, produces an output with the desired gust PSD.[6] A general state-space realization of such filter is

$$\{\dot{x}_g\} = [A_g]\{x_g\} + \{B_g\}w \qquad \{y_g\} = [C_g]\{x_g\} + \{D_g\}w \tag{4}$$

where the output $\{y_g\}$ is the gust input $\{w_p\}$ in Eq. (2), and w is a white-noise signal. Since the PSD functions of w_g vanish when $\omega \to \infty$, the only term in $\{D_g\}$ that may be nonzero is the one associated with $\dot{w}_g$. Augmentation of the gust states, $\{x_g\}$ of Eq. (4) to the aeroservoelastic states, $\{x_p\}$ of Eq. (2), yields

$$\{\dot{x}\} = [A]\{x\} + \{B_w\}w \tag{5}$$

where

$$\{x\} = \begin{Bmatrix} x_p \\ x_g \end{Bmatrix}, \qquad [A] = \begin{bmatrix} [A_p] & [B_{w_p}][C_g] \\ 0 & [A_g] \end{bmatrix}$$

$$\{B_w\} = \begin{Bmatrix} [B_{w_p}]\{D_g\} \\ \{B_g\} \end{Bmatrix}$$

The output Eq. (3) becomes

$$\{y\} = [C]\{x\} + \{D_w\}w \tag{6}$$

where

$$[C] = [[C_p]\ [D_{w_p}][C_g]], \qquad \{D_w\} = [D_{w_p}]\{D_g\}$$

which may have a nonzero noise term when accelerations appear in the output. Since a white noise does not have a finite rms value, the acceleration response in this case may not have a finite rms either. The noise term in Eq. (6) can be eliminated in two ways: 1) designing the gust filter such that the order of the denominator is larger than the order of the numerator by 2 or more; and 2) constraining the aerodynamic approximation, Eq. (1), to yield a zero gust column in $[A_1]$, which yields $[D_{w_p}]\{D_g\} = 0$. The first way may add an extra state (as shown below), but it is preferable because the $\{A_{g_1}\} = 0$ constraint may cause an inaccurate approximation of the aerodynamic gust column.

The gust filter suggested in Ref. 6 to represent Dryden's gust can be described by the transfer function

$$T_g(s) \equiv w_g(s)/w(s) = \sigma_{w_g}(\sqrt{3}\tau_g^{-1/2}s + \tau_g^{-3/2})/(s + \tau_g^{-1})^2 \tag{7}$$

where σ_{w_g} is the rms value of the gust velocity, and where $\tau_g = L_g/V$, where L_g is the scale of turbulence. Since $\dot{w}_g$ is included in $\{y_g\}$ of Eq. (4), the state-pace realization of this gust filter would have a nonzero $\{D_w\}$. To allow the computation of acceleration response, $T_g(s)$ is modified by a low-pass filter

$$\bar{T}_g(s) = [a/(s + a)]T_g(s) \tag{8}$$

where a is chosen to be well above the maximum natural frequency taken into account. A state-space realization of $\bar{T}_g(s)$ is Eq. (4) with

$$[A_g] = \begin{bmatrix} 0 & 1 & 0 \\ -\tau_g^{-2} & -2\tau_g^{-1} & a \\ 0 & 0 & -a \end{bmatrix}, \quad \{B_g\} = \begin{Bmatrix} 0 \\ 0 \\ \sigma_{w_g} \end{Bmatrix}, \quad \{D_g\} = \{0\}$$

$$[C_g] = \begin{bmatrix} \tau_g^{-3/2} & \sqrt{3}\tau_g^{-1/2} & 0 \\ -\sqrt{3}\tau_g^{-5/2} & (1 - 2\sqrt{3})\tau_g^{-3/2} & \sqrt{3}a\tau_g^{-1/2} \end{bmatrix} \tag{9}$$

The von Kármán PSD, which is a nonrational function of ω, can also be approximated by a rational transfer function[1] that, with the low-pass filter of Eq. (8), leads also to a state-space representation with no noise term in the output. With $\{D_g\} = \{0\}$, $[B_{w_g}]\{D_g\}$ in $\{B_w\}$ of Eq. (5) is eliminated as well. Consequently, the only nonzero part of $\{B_w\}$ is σ_{w_g}, which is independent of the design variables.

Response and Sensitivity Derivatives

Root-mean-square values of the response parameters are based on the state covariance matrix $[X] \equiv E[\{x\}\{x\}^T]$. When Eq. (5) is excited by a unit-intensity white noise, $[X]$ satisfies the matrix Lyapunov equation[10]

$$[A][X] + [X][A]^T = -\{B_w\}\{B_w\}^T \tag{10}$$

A unique solution for $[X]$ is obtainable when the real parts of all the roots of $[A]$ are not zero. Neutral-stability rigid body modes (such as heave) yield a singular $[A]$, namely a zero root, at all dynamic pressures. Unless modified by the control system, the singularity is eliminated by removing the columns and rows in $[A]$ that are associated with the displacements of these modes while retaining their velocity states. The covariance matrix associated with $\{y\}$ of Eq. (6), with zero noise, is

$$[Y] \equiv E[\{y\}\{y\}^T] = [C][X][C]^T \tag{11}$$

The diagonal of $[Y]$ contains the mean-square output response parameters σ_y^2. Off-diagonal terms in $[Y]$ may be used to define equal-probability ellipses[1] of y_i and y_j, which are based on the autocorrelations Y_{ii} and Y_{jj} and the cross-correlation coefficient $\rho_{ij} = Y_{ij}/\sqrt{Y_{ii}Y_{jj}}$.

An automated design process with gust response considerations requires the sensitivity derivatives of response parameters with respect to the design variables. The first step in obtaining these derivatives is the computation of the derivatives of the system matrices $[A]$ and $[C]$ of Eqs. (5) and (6). The optimization approach in this work is that of Ref. 8. The system matrix sensitivity derivatives are formulated in Ref. 11.

The differentiation of the matrix Lyapunov Eq. (10) with respect to a design variable p, using $\partial\{B_w\}/\partial p = 0$, yields another Lyapunov equation

$$[A]\frac{\partial[X]}{\partial p} + \frac{\partial[X]}{\partial p}[A]^T = -\frac{\partial[A]}{\partial p}[X] - [X]\frac{\partial[A]^T}{\partial p} \tag{12}$$

which can be solved for $\partial[X]/\partial p$. A new solution is required for each design variable, but they can all be based on the same decomposition used in solving for $[X]$ by Eq. (10). The differentiation of Eq. (11) yields the response sensitivity derivatives

$$\frac{\partial[Y]}{\partial p} = [C]\frac{\partial[X]}{\partial p}[C]^T + \frac{\partial[C]}{\partial p}[X][C]^T + [C][X]\frac{\partial[C]^T}{\partial p} \tag{13}$$

where the diagonal terms, $\partial\sigma_y^2/\partial p$, are usually the only derivatives of interest.

Numerical Example

The numerical example is based on the jet transport model that was also used as a sample problem HA76C for MSC/NASTRAN.[12] One rigid-body mode (in heave) and 11 elastic modes are used to represent the structure (23 states). The control system reads the acceleration response at the wingtip and drives a trailing-edge control surface through a low-pass filter and a third-order actuator (4 control states). The gust filter represents Dryden's gust, Eq. (7) with $\tau_g = 3.6$ s and

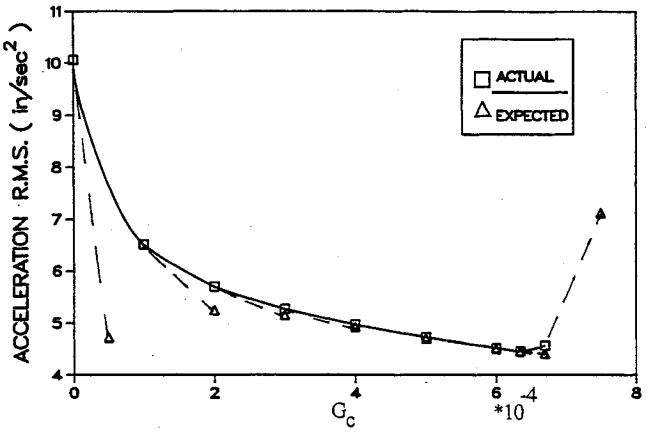

Fig. 1 Closed-loop wingtip rms acceleration vs control gain.

$\sigma_{w_g} = 1$ in./s, premultiplied by the low-pass filter of Eq. (8) with $a = 2640$ rad/s, which yields 3 gust states.

Fifteen doublet-lattice unsteady AFC matrices were calculated at Mach 0.62 for k values of 0 to 4.0. The MS aerodynamic approximation, Eq. (9), was performed with 4 aerodynamic lag terms that yield 4 aerodynamic states. The initial constraint set was data matched at $k = 0.0$ and $k = 4.0$, which is well above the frequencies of significant aeroelastic activity. To evaluate the accuracy of the aerodynamic approximation in gust-response analysis, PSD functions of the response were calculated in the frequency domain once with the "exact" quadratic interpolation of the tabulated AFC matrices via MSC/NASTRAN, and once with the MS approximated aerodynamics. While the PSD functions of wingtip acceleration—obtained by the two ways—were in excellent agreement, the MS wing-root bending-moment exhibited large errors in the range of 0–0.3 Hz. The errors are related to inaccuracies in approximating the quasisteady aerodynamics associated with rigid-body vertical velocity. The problem was fixed by constraining the approximation to match the imaginary data at the lowest nonzero tabulated $k = 0.005$ instead of the imaginary-part match at $k = 4$. The change had negligible effects of other results.

Parametric studies were performed at 90% of the open-loop flutter dynamic pressure to demonstrate gust response and sensitivity variations with structural and control design variables. An example is the effect of the preactuator control gain G_c on the wingtip acceleration response, shown in Fig. 1. The "expected" values in the figure, which are based on the sensitivity derivatives at the connected points, demonstrate the accuracy of the sensitivity computations. A separate analysis indicated 3.0-Hz flutter with $G_c = -0.4 \times 10^{-4}$. It can be observed in Fig. 1 that the control law is very effective at low positive gain values. When the gain increases, the system approaches a 30.4-Hz flutter at $G_c = 6.8 \times 10^{-4}$. The two flutter bounds are indicated in Fig. 1 by the large sensitivity derivatives at $G_c = 0.0$ and $G_c = 6.7 \times 10^{-4}$.

References

[1]Hoblit, F. M., *Gust Loads on Aircraft: Concepts and Applications*, AIAA Education Series, AIAA, Washington, DC, 1988.

[2]Roger, K. L., "Airplane Math Modeling and Active Aeroelastic Control Design," AGARD, Neuilly Sur Seine, France, 1977, pp. 4.1–4.11 (AGARD-228).

[3]Karpel, M., "Design for Active Flutter Suppression and Gust Alleviation Using State-Space Aeroelastic Modeling," *Journal of Aircraft*, Vol. 19, No. 3, 1982, pp. 221–227.

[4]Karpel, M., "Time Domain Aeroservoelastic Modeling Using Weighted Unsteady Aerodynamic Forces," *Journal of Guidance, Control, and Dynamics*, Vol. 13, No. 1, 1990, pp. 30–37.

[5]Hoadley, S. T., and Karpel, M., "Application of Aeroservoelastic Modeling Using Minimum-State Unsteady Aerodynamic Approximations," *Journal of Guidance, Control, and Dynamics*, Vol. 14, No. 6, 1991, pp. 1267–1276.

[6]Mukhopadhyay, V., Newsome, J. R., and Abel, I., "A Method for Obtaining Reduced-Order Control Laws for High-Order Systems Using Optimization Techniques," NASA TP-1876, 1981.

[7]Livne, E., Schmit, L. A., and Friedmann, P. P., "Towards Integrated Multidisciplinary Synthesis of Actively Controlled Fiber Composite Wings," *Journal of Aircraft*, Vol. 27, No. 12, 1990, pp. 979–992.

[8]Karpel, M., "Multidisciplinary Optimization of Aeroservoelastic Systems Using Reduced Size Models," *Journal of Aircraft*, Vol. 29, No. 5, 1992, pp. 939–946.

[9]Karpel, M., "Size-Reduction Techniques for the Determination of Efficient Aeroservoelastic Models," *Control and Dynamic Systems*, edited by C. Leondes, Vol. 54, Academic Press, San Diego, CA, 1992, pp. 263–295.

[10]Bryson, A. E., and Ho, Y. C., "Applied Optimal Control," Hemisphere, Washington, DC, 1975.

[11]Karpel, M., "Sensitivity Derivatives of Flutter Characteristics and Stability Margins for Aeroservoelastic Design," *Journal of Aircraft*, Vol. 27, No. 4, 1990, pp. 368–375.

[12]"Handbook for Aeroelastic Analysis," MSC/NASTRAN Version 65, The MacNeal-Schwendler Corp., Los Angeles, CA, 1987.

Interference Between Tanker Wing Wake with Roll-Up and Receiver Aircraft

A. W. Bloy* and M. G. West†
University of Manchester,
Manchester M13 9PL, England, United Kingdom

Introduction

VORTEX wake roll-up is a problem of interest when one aircraft flies in formation behind another aircraft as in air-to-air refueling. In this case the following or receiver aircraft approaches the leading or tanker aircraft from below, and typically refuels at a position about one span downstream of the tanker aircraft. A more detailed description of the approach has been given by Bradley[1] for the hose and drogue method of refueling, and by Hoganson[2] for the flying boom method of refueling. During refueling, the main wing of the receiver lies below the tanker wake trailing vortices, although the fin may intersect the tanker wake.

In a previous work, Bloy et al.[3–5] investigated both theoretically and experimentally the effect of the tanker downwash and sidewash on the receiver. Relatively simple wake models were used and it is the purpose of this Note to present results for a more realistic roll-up model of the wake. There are numerous other references on vortex roll-up, although many of these are two-dimensional methods applicable far downstream of the wing. For the present case a method that allows for the effect of the wing bound vortices was required. Also, it was not considered necessary to correctly model the trailing vortex viscous core since the flow of interest is that well outside the core. The chosen method is similar to that used by Butter and Hancock[6] in which the trailing vortex sheet is represented by vortex lines shed from the wing trailing edge. The positions of these vortex lines are then determined by integrating downstream. Moore[7] found that the line vortex method can produce chaotic motion of the vortices associated with the very high velocities induced by vortices in close prox-

Received May 23, 1993; revision received Aug. 16, 1993; accepted for publication Sept. 3, 1993.

*Lecturer, Department of Engineering.
†Research Assistant, Department of Engineering.